

pubs.acs.org/acscatalysis Research Article

Multi-State Living Degenerative and Chain Transfer Coordinative Polymerization of α -Olefins via Sub-Stoichiometric Activation

Mark A. Wallace and Lawrence R. Sita*



Cite This: ACS Catal. 2021, 11, 9754-9760



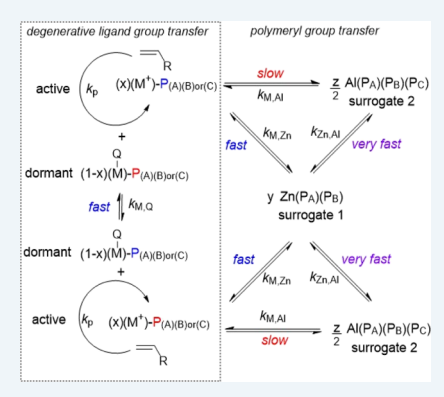
ACCESS

Metrics & More

Article Recommendations

Supporting Information

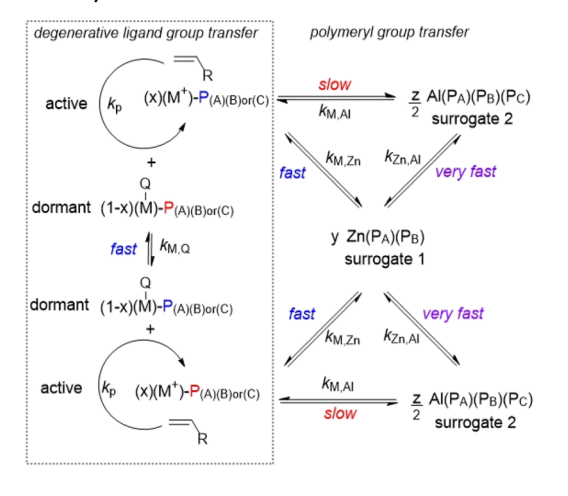
ABSTRACT: Sub-stoichiometric activation of a transition-metal pre-initiator by a borate coinitiator in the presence of excess equivalents of a single or two different types of maingroup-metal alkyls provides the basis for the mechanistically complex, but highly effective, multi-state degenerative living coordinative chain transfer polymerization (MSD-LCCTP) of α-olefins. By controlling the relative rates of group and chain transfers between active, dormant, and surrogate species, MSD-LCCTP can be directed to provide polyolefin products with a tunable degree of polymerization and a tunable molecular weight distribution. Further, the ability to use as little as 0.25 equiv of the borate coinitiator with a large excess of mixtures of ZnEt₂/AlEt₃ in varying ratios as surrogate chain growth centers greatly increases the scalability of MSD-LCCTP for providing practical quantities of next-generation polyolefins.



KEYWORDS: living, degenerative, chain transfer, polymerization, polyolefin

olyolefins are remarkable in terms of the diversity of materials that are available from the very small set of industrially relevant olefin monomers, as well as the incredible array of different products and applications that they support. Unfortunately, at over 300 million metric tons produced each year (and growing), polyolefins also comprise the single largest component of global plastic waste.2 Accordingly, there is the need and desire to design and develop the next generation of polyolefins that can continue to support the technological needs of society while also serving to reduce future environmental impacts.3 To achieve this goal, highly versatile polymerization processes must also be designed and developed that can deliver new structural forms of polyolefins in a programmable way and, importantly, in a manner that is not supply- or cost-prohibitive. Herein, we present the results of a successful program to validate a new olefin polymerization process that we term multi-state degenerative living coordinative chain-transfer polymerization (MSD-LCCTP). As shown in Scheme 1, the foundations of MSD-LCCTP begin with our previously reported two- and three-state LCCTP processes that operate through a fast and reversible polymeryl group (chain) transfer that occurs between a population of active transition-metal propagators and much larger populations of inactive main-group-metal alkyl species that serve as surrogate chain growth centers.⁵ The new twist for MSD-LCCTP is that the transition-metal pre-initiator is now activated by only a sub-stoichiometric amount of the required coinitiator to establish an additional population of inactive transition-metal dormant species that are also in exchange with the active propagator through a fast and reversible ligand group

Scheme 1. Mechanistic Details of MSD-LCCTP for the Case of Three-State LCCTP in Which the Pre-initiator Is Activated by a Sub-Stoichiometric Amount of Coinitiator



If $v_{M,Q}$ $(k_{M,Q}) > v_{Zn,AI}$ $(k_{Zn,AI}) > v_{M,Zn}$ $(k_{M,Zn}) > v_{M,AI}$ $(k_{M,AI})$, then

$$DP_{n} = \underbrace{\text{[monomer]}_{(t-0)}}_{\text{[fpre-initiator} + 2y(ZnP_{2}) + 3z(AlP_{3})]}; D \approx 1 + \frac{k_{p}}{k_{app}}; \underbrace{\text{Cost of}}_{\text{scaling}} \propto \begin{pmatrix} y \text{ ZnEt}_{2} + z \text{ AlEt}_{3} \\ + x \text{ co-initiator} \\ + \text{ pre-initiator} \end{pmatrix}$$

Received: May 11, 2021 **Revised:** July 5, 2021 **Published:** July 19, 2021





(Q) transfer, which is a component part of degenerative living coordinative polymerization (LCP) according to the boxed area of Scheme 1.^{6,7} At first glance, the challenge of coordinating all the various kinetic parameters associated with the apparent daunting complexity of MSD-LCCTP would seem to negate any potential benefits of using it to produce unique polyolefins. However, in the present report, we not only demonstrate that this can be easily achieved with existing materials and methods but also that the increased complexity of MSD-LCCTP is advantageous for providing new external controls that can be used to further expand the range of polyolefin grades that are obtainable from a single olefin monomer, which also significantly lowers the costs associated with the scale-up of this process to provide practical quantities of the product.

To begin, LCP of ethene, α -olefins, and α , ω -nonconjugated dienes is attractive for providing access to a wide range of new structural forms of polyolefin materials, some of which display technologically interesting properties. 3a,8 On the other hand, the "one chain per active site" limitation that is a characteristic feature of all living polymerizations is particularly problematic for LCP, where the weight fraction of the chain can be relatively small vis-à-vis the total molar mass of the active cationic transition-metal propagator, which is also most often an ion pair with an associated counteranion of substantial molecular weight. For LCCTP, if the rate and the rate constant of chain transfer between active transition-metal (M) and surrogate main-group-metal (M') chain growth centers, $\nu_{\mathrm{MM'}}$ and $k_{M,M'}$, respectively, are much greater in magnitude than the corresponding kinetic parameters for propagation, $\nu_{\rm p}$ ($k_{\rm p}$), then, in the absence of irreversible chain termination, all the desired attributes of LCP can still be achieved. These features include having a tunable number-average degree of polymerization, DP_n, and a very narrow molecular weight distribution (MWD), as defined by the dispersity index, $D = M_w/M_n \approx 1 +$ $k_{\rm p}/k_{\rm M,M'}$, where $M_{\rm n}$ and $M_{\rm w}$ are the number- and weight-average molecular weight indices, respectively. 9,10 However, the cost of scale-up is now carried by that of a relatively inexpensive commodity main-group-metal alkyl, such as diethylzinc (ZnEt₂), triethylaluminum (AlEt₃), or a mixture of the two, that is present in an excess amount at the start of LCCTP. In this regard, AlEt₃ as the chain-transfer agent (CTA) is most preferred over ZnEt₂ due to a lower pricing and greater safety in transport and handling. On the other hand, for two-state LCCTP (i.e., chain transfer involving only the active propagator and a single type of surrogate species), $\nu_{
m M,Al}$ and $k_{
m MAl}$ are substantially smaller in magnitude than $u_{
m M.Zn}$ and $k_{
m M,Zn}$, and this manifests as a much broader MWD and larger Dvalue for AlEt₃ versus ZnEt₂ as the source of the surrogate chain growth centers. To ameliorate this difference, we have previously shown that due to a very facile reversible chain transfer between Zn and Al, the addition of a small amount of ZnEt₂ to the original AlEt₃-mediated process serves to establish three-state LCCTP (i.e., chain transfer between the active propagator and two different types of surrogate species) for which both the MWD and D value are close to those obtained by using ZnEt₂ alone as the CTA. 5c,11 However, this previous study did not establish the ability to fine-tune MWD and D as a function of the AlEt₃/ZnEt₂ ratio.

In addition to cost considerations, two- and three-state LCCTP are ideally suited for the scaled production of low to ultra-low-molecular-weight polyolefins with small DP_{n} values that are below the minimum chain entanglement length. ⁴ The

reactive quenching of LCCTP through the addition of a variety of inexpensive X-Y reagents (e.g., I_2 and O_2) can also provide high yields of quantitative end-group-functionalized poly(α olefinates) (x-PAOs) for which the occupied free volume can be manipulated through the judicious design of DP_n and the steric bulk of the α -olefin (e.g., propene vs 1-hexene vs 4methyl-1-pentene). 12 This new category of x-PAO materials also finds use as hydrophobic building blocks for the design of amphiphilic conjugates that undergo self-assembly in the condensed phase to provide a variety of thermotropic canonical and non-canonical highly ordered nanostructured phase morphologies.¹³ However, the further development of LCCTP as a synthetic strategy and tool for obtaining practical quantities of new fundamental forms of polyolefins is still held back by the amount of the coinitiator that is required to establish the population of active propagators from the transition-metal pre-initiator. Indeed, in the present work, the coinitiator is the well-known dimethylanilinium perfluorinated tetra-aryl borate, [PhNHMe₂][B(C₆F₅)₄] (B1), and the cost of this reagent becomes a key limiting factor for scalability.¹⁴ Another issue with B1, and related borane and borate coinitiators, is the need to purify the product and dispose of the chemical waste associated with the $[B(C_6F_5)_4]$ anion. Accordingly, while we are exploring the development of "greener" coinitiators for LCCTP, in the interim, we have sought to determine the minimum amount of the coinitiator that is required to provide the same polyolefin product. This goal then raised the question of the possibility of using a substoichiometric amount relative to that of the pre-initiator.

We have previously reported that the sub-stoichiometric activation of a transition-metal pre-initiator by a coinitiator can be used for the degenerative $\hat{L}CP$ of α -olefins that proceeds according to the boxed mechanism of Scheme 1.6,15 More specifically, by employing less than one full equivalent of the coinitiator to activate a neutral $L_nM(Q)_2$ (Q = Me, Cl) preinitiator through the abstraction of one of the Q ligands, a system for degenerative LCP is established that consists of a population of x active propagators and a population of (1-x)dormant species that are in dynamic exchange through a fast and reversible group transfer of the remaining Q ligand (see Scheme 1). Just as in the case of LCCTP, if the rate and the rate constant for Q group exchange, $\nu_{M,Q}$ ($k_{M,Q}$), are far greater than those for propagation, $\nu_{\rm p}$ ($k_{\rm p}$), then all the active and dormant species will appear to undergo chain growth at the same rate, and both DP_n and D will remain unchanged relative to the values one would have obtained using a full stoichiometric equivalent of the coinitiator. Although not relevant for the present study, we have also shown that one can capitalize on the relative configurational stability of chiral, C_1 symmetric active and dormant species under degenerative LCP conditions to "stereoengineer" the microstructure tacticity of polyolefins through the programed introduction of different levels of stereoerrors. 6e,f,h,i Finally, we have demonstrated that the degenerative LCP of α -olefins can be effectively performed for both cases of Q = Me and Cl and with as little as 0.25 equiv of a borate coinitiator.

Our past success with degenerative LCP and the need to further define the conditions under which practical and scalable two- and three-state LCCTP can be conducted naturally led us to consider if MSD-LCCTP can work as envisioned in Scheme 1. Here, it can be noted that in addition to the need for all the relative magnitudes of the kinetic parameters for the reversible and irreversible processes to fall

into place, the success of MSD-LCCTP requires that no new deleterious interactions occur between the dormant and surrogate species, which is not possible to predict *a priori*. As will be shown, these concerns did not materialize into any issue that could not be resolved and indeed, MSD-LCCTP not only proved to be very easy to perform using our existing collection of pre-initiators and coinitiators but we were also additionally able to demonstrate its utility for fine-tuning the MWD and D values to produce a family of different grades of a polyolefin using a single α -olefin (*vide infra*).

Scheme 2 provides a summary of the method and materials used to validate MSD-LCCTP that is mechanistically outlined

Scheme 2. Methods and Materials Used to Evaluate MSD-LCCTP of 1-Hexene

1 eq. 1

$$x \neq q$$
. B1
 $y \neq q$. ZnEt₂
 $z \neq q$. AlEt₃

poly(1-hexene) (PH)

Me

B1 = [PhNHMe₂][B(C₆F₅)₄]

in Scheme 1. For this study, the cyclopentadienyl, amidinate (CPAM) hafnium dimethyl complex, $Cp^*[N(Et)C(Me)C-(Et)]HfMe_2$ ($Cp^*=\eta^5-C_5Me_5$) (1), was selected because we have previously shown that, in combination with a stoichiometric amount of the coinitiator **B1**, it can be used for both the LCP and the two- and three-state LCCTP of ethene, propene, higher carbon-numbered linear and branched α -olefins, and α , ω -nonconjugated dienes. Table 1 further provides a summary of the experiments performed using 1-hexene as the α -olefin monomer with different amounts of **B1** and the main-group-metal alkyls, ZnEt₂ and AlEt₃. Finally, Table 1 includes the results obtained for the characterization of the atactic poly(1-hexene) (aPH) products by gel permeation chromatography (GPC).

Although the initiator derived from 1 and a stoichiometric amount of B1 have been shown to be competent for the LCP of 1-hexene, there are several potential problems that can arise when attempting to perform degenerative LCP at less than a 100% level of activation. More to the point, our previous

studies with degenerative LCP employed the related C_1 -symmetric CPAM zirconium derivative, $Cp^*[N(Et)C(Me)C^{t}Bu)]ZrMe_2$ (2), which has a more sterically shielded metal center than 1. Even so, the ion-pair initiator derived from 2 and B1 can dimerize in the solid state to form the crystallographically characterized bimetallic $bis(\mu\text{-Me})$ -bridged complex, $\{Cp^*[N(Et)C(Me)C({}^tBu)]Zr(\mu\text{-Me})\}_2\{[B-(C_6F_5)_4]\}_2$ (3). We have also reported on the observation that an increase in the population of dormant species relative to active species retards the overall apparent rate of propagation potentially due to the reversible formation of inactive bimetallic μ -Q-bridged species, such as 4, that is shown in Scheme 3. Accordingly, from the outset of this study, it was unclear if the combination of 1 and a substoichiometric amount of B1 would be viable for degenerative LCP.

Scheme 3. Proposed Inactive Bimetallic μ -Q-Bridged Intermediate Formed between an Active Propagator and Dormant Species under Degenerative LCP

Runs 1 and 2 of Table 1 provide the conditions and results for the LCP of 1-hexene using 1 activated by B1 at 100 and 50% levels, respectively. After the usual acidic quench and workup, GPC analysis revealed nearly identical yields and $M_{\rm n}$ values for the two respective aPH samples. However, while a monomodal and narrow MWD was observed in each case, the D value of the aPH from run 2 was seen to be slightly larger than that of run 1 (cf. 1.29 vs 1.19 in Table 1). We attribute this result as arising from the rate constant for the methyl group exchange now being a major determinant of dispersity at a 50% level of activation (see Scheme 1). It can also be noted here that the GPC characterization of the set of 13 narrow polystyrene (PS) standards used to generate the calibration curve under identical conditions used for analysis of the aPH samples of Table 1 consistently provided slightly

Table 1. LCP and MSD-LCCTP of 1-Hexene

			/		- (2 -)	(*)	()			- 0
run	equiv ^a (g) 1-hexene	B1 (equiv)	$ZnEt_2$ (equiv)	AlEt ₃ (equiv)	T (°C)	$t_{\rm p}$ (h)	yield (g)	$M_{\rm n}^{\ e}$ (Da)	$M_{\rm w}^{\ e}$ (Da)	D^e
1 ^b	178 (0.6)	1.10			-5	10	0.6	24,520	29,170	1.19
2^{b}	178 (0.6)	0.50			-5	10	0.6	21,670	27,370	1.26
3 ^c	1900 (3.2)	1.10	20		25	24	2.9	3,960	4,630	1.17
4 ^c	1900 (3.2)	0.50	20		25	24	3.0	3,710	4,440	1.20
5 ^d	1900 (6.4)	0.25	20		25	24	4.5	3,190	3,780	1.19
6 ^c	1900 (3.2)	0.50	20		-5	24	3.1	4,310	5,060	1.17
7 ^c	1900 (3.2)	0.50	20		40	18	1.9	2,410	3,300	1.37
8 ^c	1900 (3.2)	0.50		13.40	25	24	3.1	8,240	20,870	2.53
9 ^c	1900 (3.2)	0.50	3.0	11.30	25	24	2.9	4,170	5,180	1.24
10^{c}	1900 (3.2)	0.50	2.0	12.00	25	24	2.8	3,020	3,790	1.26
11 ^c	1900 (3.2)	0.50	1.0	12.67	25	24	3.0	3,940	5,110	1.30
12 ^c	1900 (3.2)	0.50	0.5	13.01	25	24	2.9	4,170	5,700	1.37

[&]quot;Molar equivalents relative to 1. $^b40~\mu$ mol of 1 in 5 mL of chlorobenzene. $^c20~\mu$ mol of 1 in 5 mL of toluene. $^d40~\mu$ mol of 1 in 5 mL of toluene. c Determined by GPC (relative to 13 PS standards).

lower $M_{\rm n}$ and higher D values than those stated by the commercial source [cf., for PS-6: $M_{\rm n}=4740$ Da, D=1.03 (sourced) vs $M_{\rm n}=4124$ Da, D=1.16 (experimental)]. Finally, 1 H and 13 C{ 1 H} NMR spectra for both aPH samples confirmed an atactic stereochemical microstructure as expected, as well as the living character of these coordination polymerization by showing the absence of vinylidene resonances that might have arisen from chain termination occurring through β -hydrogen transfer.

Having established that degenerative LCP of 1-hexene can be successfully achieved using sub-stoichiometric activation of 1 by B1, the next step was to show that the reversible methyl group exchange between the active and dormant species does not interfere with the reversible chain transfer that is mediated by surrogate chain growth centers. Thus, runs 3, 4, and 5 of Table 1 were performed to determine the possible effects on the aPH products obtained from MSD-LCCTP as a function of decreasing the level of activation in the presence of a fixed amount of 20 equiv of ZnEt₂ (i.e., 40 equiv of transferable Et groups). The polymerization temperature was also increased from -5 to 25 °C in order to facilitate faster exchange and overall propagation rates. As shown in Table 1, the yields of aPH for runs 3 and 4 were high at 90 and 93%, respectively, while, for the same polymerization time, that for run 5 was significantly less at 70%. GPC analysis of all three aPH materials also revealed that $M_{\rm n}$ values for runs 3 and 4 were nearly identical, while for run 5, a significant drop had once again occurred (see Table 1). On the other hand, all three D values are shown to be very small and virtually independent of % activation and as reproduced in Figure 1, the MWDs

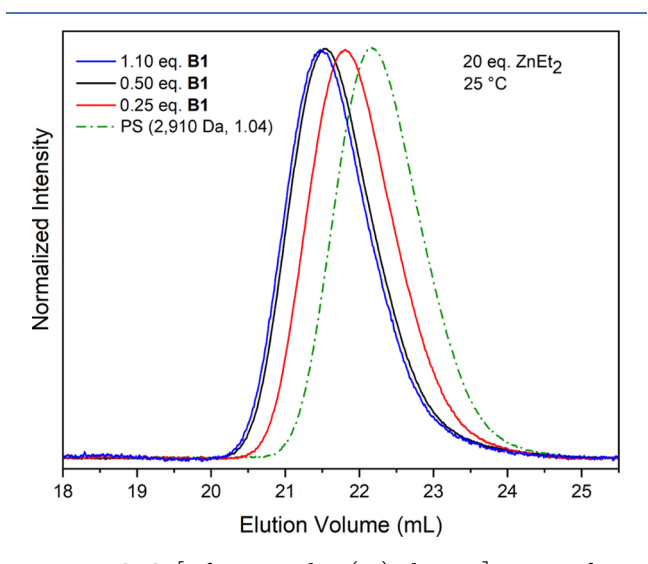


Figure 1. GPC [refractive index (RI) detector] traces of aPH obtained from runs 3–5 of Table 1. A GPC trace for a PS standard (PS-5: $M_{\rm n}=2910$ Da and D=1.04) analyzed using the same system is provided for comparison.

remained very narrow and monomodal. We attribute these observations as arising from a decrease in the overall apparent rate of propagation due to a steady decrease in the total number of active sites as well as the reversible formation of an inactive bimetallic μ -Me-bridged intermediate similar to that of 4 shown in Scheme 3 that is favored at high concentrations of dormant species. On the other hand, this rate retardation that becomes significant at low % activation does not appear to have any effect on the living character of polymerization.

We next explored the effect of temperature on the MSD-LCCTP of 1-hexene with runs 6 and 7 being performed at -5 and 40 °C, respectively, and with 50% activation of 1 and in the presence of 20 equiv of ZnEt₂. Table 1 and Figure 2

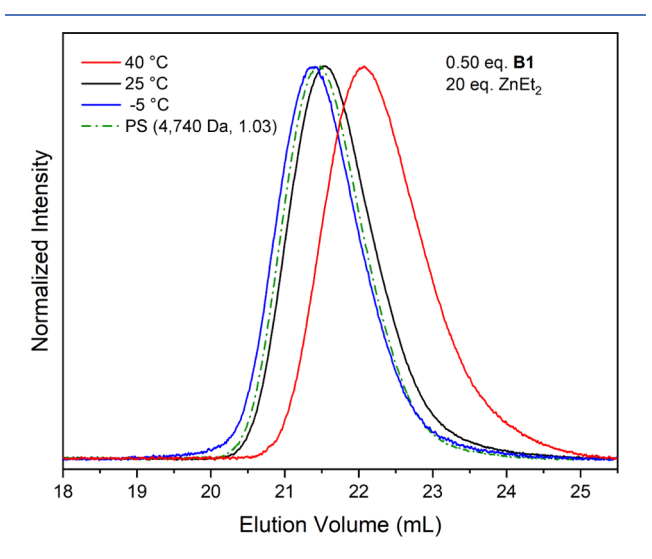


Figure 2. GPC (RI detector) traces of aPH obtained for runs 4, 6, and 7 of Table 1. A GPC trace for a PS standard (PS-6: M_n = 4740 Da and D = 1.03) analyzed using the same system is provided for comparison.

provide details of the yields and GPC determined $M_{\rm n}$, $M_{\rm w}$, and B values of the aPH products that, along with the MWD profiles, can be compared to the results for the aPH obtained at 25 °C under identical conditions (run 4). As can be seen, there is very little effect on these parameters in going from -5 °C (run 6) to 25 °C (run 4), which is to be expected. On the other hand, an increase to 40 °C had a deleterious impact on both yield and dispersity (cf. B = 1.36), and the small degree of asymmetry in the MWD that appears in Figure 2 favoring the low molecular side strongly suggests that polymerization is no longer strictly living at this temperature. In support of this conclusion, a 1 H NMR spectrum of the aPH material from run 7 now revealed the presence of vinylidene resonances that most likely originate from chain-termination by a β -hydrogen transfer process. 16

As mentioned previously, there are key advantages to using AlEt₃ rather than ZnEt₂ as the source of surrogate chain growth centers in terms of overall cost and safety. However, the key disadvantage of this CTA for LCCTP lies in the reduced kinetic parameters for reversible chain transfer between the Hf and Al metal centers that gives rise to much broader MWDs for the polyolefin products. It can be further anticipated that, due to the known stability of the $[{\rm Et_2Al}(\mu$ -Et)]₂ dimer in solution, that MSD-LCCTP conducted with the sub-stoichiometric activation of 1 using only AlEt3 as the CTA might lead to the formation of inactive or chain-terminating Hf/Al heterobimetallic species. 18 Accordingly, run 8 of Table 1 provides a critical benchmark for the MSD-LCCTP of 1hexene in which 13.4 equiv of AlEt₃ (40 equiv of transferable Et groups) were used in combination with a 50% level of activation of 1 at 25 $\,^{\circ}$ C. In addition, gratifyingly, for the same period of time, the yield of aPH obtained was nearly the same as when 20 equiv of ZnEt₂ were used (cf. run 4). However, as Table 1 and Figure 3 additionally reveal, a substantially broader MWD with a D value of 2.53 for this aPH material is now confirmed by GPC. Because NMR spectroscopy did not

ACS Catalysis pubs.acs.org/acscatalysis Research Article

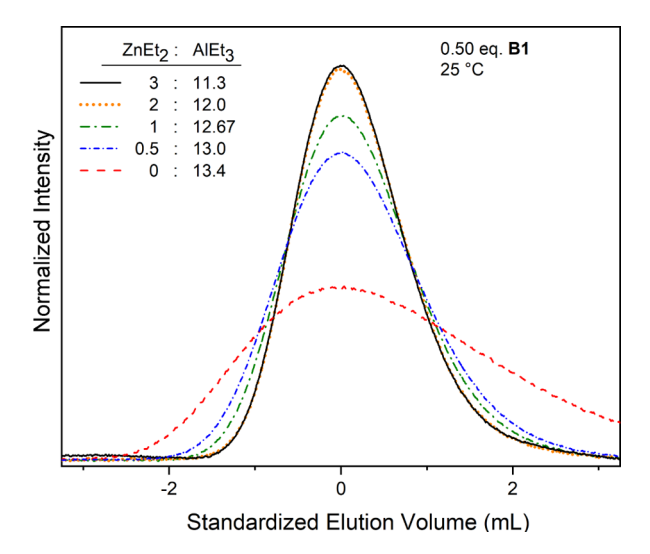


Figure 3. GPC (RI detector) traces of aPH obtained for runs 8–12 of Table 1. The elution volumes are standardized with respect to the maxima for the sake of highlighting the differences in the MWD profiles, and maxima heights are normalized with respect to a constant MWD area.

provide any evidence for chain termination by β -hydrogen transfer, it can be concluded from these collective results that, although the degenerative methyl group exchange is not impeded by either the initial or surrogate trialkylaluminum species, AlP₃ (P = Et or polymeryl), that are present, it is once again slow reversible Hf \Leftrightarrow Al chain transfer kinetics relative to propagation that is responsible for the broad MWD profile.

Recently, there has been significant interest in developing polymerization processes that can be used to modulate the MWD profiles of different classes of polymers because this structural feature plays an important role in defining the physical properties and processibility that are important for technical applications. ¹⁹ In this regard, we have also recently demonstrated the ability to use temporal control over the addition of successive portions of CTAs during the two- and three-state LCCTP of a variety of α -olefins as a means by which to program different targeted MWD profiles for the polyolefin products, including variations in breadth, asymmetry, and modal nature (e.g., mono-, bi-, and multi-modal). ²⁰

For MSD-LCCTP, we hypothesized that it might be possible to now modulate the breadth of the MWD using different AlEt₃/ZnEt₂ ratios as a way to fine-tune the overall apparent rate constant of chain transfer, $k_{\rm app}$, relative to propagation *via* the relationship, $D \approx 1 + k_{\rm p}/k_{\rm app}$ (see Scheme 1). Thus, runs 9–12 of Table 1 were additionally performed in order to probe this conjecture and gratifyingly, the yields and GPC data obtained and presented in the table and Figure 3 appear to validate the use of MSD-LCCTP for this purpose. More specifically, for each run, the AlEt₃/ZnEt₂ ratio was adjusted to have a decreasing amount of ZnEt2 in the initial mixture of CTAs but with the total number of transferable Et groups remaining constant at 40. As hoped for, a significant number of ZnEt₂ equivalents relative to AlEt₃ as used in run 9 had the most dramatic effect in terms of now providing a much narrower MWD and significantly smaller D value vis-à-vis those of run 8. Most importantly, while the small increase in the AlEt₃/ZnEt₂ ratio of run 10 affected little change in these parameters relative to the baseline provided by run 9, the further decreasing amounts of ZnEt2 used in the ratios of runs

11 and 12 had a clear impact and produced the desired trend of increasing the breadth of the MWD and value of *D* according to the tabulated results and Figure 3. Perhaps, the most striking result of these data, however, is the demonstrated effect that a very small amount of ZnEt₂ can have on the MWD profile and polydispersity of the polyolefin product when MSD-LCCTP is performed with the sub-stoichiometric activation (*cf.* the results of run 8 *vs* run 12 in Table 1 and Figure 3).

In summary, the results presented in this report demonstrate that an increase in mechanistic complexity as represented by MSD-LCCTP can lower the barriers to scalability for the production of unique new classes of polyolefins in terms of costs, safety, and environmental impact. In addition to setting a much lower (sub-stoichiometric) limit on the amount of borate coinitiator B1 that is required, MSD-LCCTP can now employ excess equivalents of AlEt₃ with only a small amount of ZnEt₂ as co-CTA being required to maintain narrow and monomodal MWD. Finally, by adjusting the AlEt₃/ZnEt₂ ratio, MSD-LCCTP provides a new external control element that can be used to fine-tune MWD to increase the number of polyolefin grades that are possible from a single olefin monomer. Investigations are now in progress to determine the full scope and limitations of these new capabilities.

ASSOCIATED CONTENT

Supporting Information

The Supporting Information is available free of charge at https://pubs.acs.org/doi/10.1021/acscatal.1c02120.

Model parameters and results, sampled Rh and Rh-(CO)2 configurations, density of states Bader partial charges and vibrational analysis, hydroformylation and hydrogenation pathways, images of optimized structures, coordinates of intermediates and transition states, and complete spectroscopic data (PDF)

AUTHOR INFORMATION

Corresponding Author

Lawrence R. Sita — Laboratory for Applied Catalyst Science and Technology, Department of Chemistry and Biochemistry, University of Maryland, College Park, Maryland 20742, United States; orcid.org/0000-0002-9880-1126; Email: lsita@umd.edu

Author

Mark A. Wallace – Laboratory for Applied Catalyst Science and Technology, Department of Chemistry and Biochemistry, University of Maryland, College Park, Maryland 20742, United States

Complete contact information is available at: https://pubs.acs.org/10.1021/acscatal.1c02120

Notes

The authors declare the following competing financial interest(s): The corresponding author has a financial interest in the university spin-out company, Precision Polyolefins, LLC (PPL). This work did not involve any PPL personnel, funding, or other resources and all new intellectual property has been disclosed in accordance with state and fed-eral requirements.

ACS Catalysis pubs.acs.org/acscatalysis Research Article

■ ACKNOWLEDGMENTS

Support of this work was provided by the National Science Foundation (CHE-1955730) for which we are grateful.

REFERENCES

- (1) (a) Handbook of Polyolefins; Vasile, C., Ed.; Marcel Dekker, Inc.: New York, 2000. (b) Polyolefins: 50 years after Ziegler and Natta I: Polyethylene and Polypropylene. In Advances in Polymer Science; Kaminsky, W., Ed.; Springer-Verlag: Heidelberg, 2013; Vol. 257. (c) Polyolefins: 50 years after Ziegler and Natta II: Polyolefins by Metallocenes and Other Single-Site Catalysts. In Advances in Polymer Science; Kaminsky, W., Ed.; Springer-Verlag: Heidelberg, 2013; Vol. 258. (d) Stürzel, M.; Mihan, S.; Mülhaupt, R. From Multisite Polymerization Catalysis to Sustainable Materials and All-Polyolefin Composites. Chem. Rev. 2016, 116, 1398–1433. (e) Polyolefin Compounds and Materials; Al-AliAlMa'adeed, M., Krupa, I., Eds.; Springer: Heidelberg, 2016.
- (2) Jubinville, D.; Esmizadeh, E.; Saikrishnan, S.; Tzoganakis, C.; Mekonnen, T. A comprehensive review of global production and recycling methods of polyolefin (PO) based products and their post-recycling application. Sustainable Mater. Technol. 2020, 25, No. e00188.
- (3) See for instance, (a) Eagan, J. M.; Xu, J.; Di Girolamo, R.; Thurber, C. M.; Macosko, C. W.; Lapointe, A. M.; Bates, F. S.; Coates, G. W. Combining polyethylene and polypropylene: Enhanced performance with PE/iPP multiblock polymers. *Science* 2017, 355, 814–816. (b) Nomura, K.; Peng, X.; Kim, H.; Jin, K.; Kim, H. J.; Bratton, A. F.; Bond, C. R.; Broman, A. E.; Miller, K. M.; Ellison, C. J. Multiblock Copolymers for Recycling Polyethylene-Poly(ethylene terephthalate) Mixed Waste. *ACS Appl. Mater. Interfaces* 2020, 12, 9726–9735.
- (4) Sita, L. R. Ex uno plures ("out of one, many"): new paradigms for expanding the range of polyolefins through reversible group transfers. *Angew. Chem., Int. Ed.* **2009**, *48*, 2464–2472.
- (5) For our prior reports of LCCTP, see: (a) Zhang, W.; Sita, L. R. Highly Efficient Living Coordinative Chain-Transfer Polymerization of Propene with ZnEt2: Practical Production of Ultrahigh to Very Low Molecular Weight Amorphous Atactic Polypropene of Extremely Narrow Polydispersity. J. Am. Chem. Soc. 2008, 130, 442-443. (b) Zhang, W.; Wei, J.; Sita, L. R. Living Coordinative Chain-Transfer Polymerization and Copolymerization of Ethene, α -Olefins, and α , ω -Nonconjugated Dienes using Dialkylzinc as "Surrogate" Chain-Growth Sites. Macromolecules 2008, 41, 7829-7833. (c) Wei, J.; Zhang, W.; Sita, L. R. Aufbaureaktion Redux: Scalable Production of Precision Hydrocarbons from AlR₃ (R = Et or iBu) by Dialkyl Zinc Mediated Ternary Living Coordinative Chain-Transfer Polymerization. Angew. Chem., Int. Ed. 2010, 49, 1768-1772. (d) Wei, J.; Zhang, W.; Wickham, R.; Sita, L. R. Programmable Modulation of Co-monomer Relative Reactivities for Living Coordination Polymerization through Reversible Chain Transfer between "Tight" and "Loose" Ion Pairs. Angew. Chem., Int. Ed. 2010, 49, 9140-9144. (e) Wei, J.; Hwang, W.; Zhang, W.; Sita, L. R. Dinuclear Bis-Propagators for the Stereoselective Living Coordinative Chain Transfer Polymerization of Propene. J. Am. Chem. Soc. 2013, 135, 2132-2135. (f) Wei, J.; Duman, L. M.; Redman, D. W.; Yonke, B. L.; Zavalij, P. Y.; Sita, L. R. N-Substituted Iminocaprolactams as Versatile and Low Cost Ligands in Group 4 Metal Initiators for the Living Coordinative Chain Transfer Polymerization of α -Olefins. Organometallics 2017, 36, 4202-4207. (g) Wallace, M. A.; Zavalij, P. Y.; Sita, L. R. Enantioselective Living Coordinative Chain Transfer Polymerization: Production of Optically Active End-Group-Functionalized (+) or (-)-Poly(methylene-1,3-cyclopentane) via a Homochiral C1-Symmetric Caproamidinate Hafnium Initiator. ACS Catal. 2020, 10, 8496-8502. (h) Cueny, E. S.; Sita, L. R.; Landis, C. R. Quantitative Validation of the Living Coordinative Chain-Transfer Polymerization of 1-Hexene using Chromophore Quench Labeling. Macromolecules 2020, 53, 5816-5825. (i) Wallace, M. A.; Wentz, C. M.; Sita, L. R. Optical Purity as a Programmable Variable for Controlling Polyolefin

- Tacticity in Living Coordinative Chain Transfer Polymerization: Application to the Stereomodulated LCCTP of α,ω -Nonconjugated Dienes. *ACS Catal.* **2021**, *11*, 4583–4592.
- (6) For our prior reports on degenerative living coordinative polymerizations proceeding by reversible (non-chain) group transfers, see: (a) Jayaratne, K. C.; Sita, L. R. Direct Methyl Group Exchange between Cationic Zirconium Ziegler-Natta Initiators and Their Living Polymers: Ramifications for the Production of Stereoblock Polyolefins. J. Am. Chem. Soc. 2001, 123, 10754-10755. (b) Zhang, Y.; Keaton, R. J.; Sita, L. R. Degenerative Transfer Living Ziegler-Natta Polymerization: Application to the Synthesis of Monomodal Stereoblock Polyolefins of Narrow Polydispersity and Tunable Block Length. J. Am. Chem. Soc. 2003, 125, 9062-9069. (c) Zhang, Y.; Sita, L. R. Stereospecific Living Ziegler-Natta Polymerization via Rapid and Reversible Chloride Degenerative Transfer between Active and Dormant Sites. J. Am. Chem. Soc. 2004, 126, 7776-7777. (d) Kissounko, D. A.; Zhang, Y.; Harney, M. B.; Sita, L. R. Evaluation of $(\eta^5 - C_5 Me_5) Hf(R)_2 [N(Et)C(Me)N(t-Bu)]$ (R = Me and i-Bu) for the Stereospecific Living and Degenerative Transfer Living Ziegler-Natta Polymerization of α -Olefins. Adv. Synth. Catal. 2005, 347, 426— 432. (e) Harney, M. B.; Zhang, Y.; Sita, L. R. Bimolecular Control over Polypropene Stereochemical Microstructure in a Well-Defined Two-State System and a New Fundamental Form: Stereogradient Polypropene. Angew. Chem., Int. Ed. 2006, 45, 6140-6144. (f) Harney, M. B.; Zhang, Y.; Sita, L. R. Discrete, Multiblock Isotactic-Atactic Stereoblock Polypropene Microstructures of Differing Block Architectures through Programmable Stereomodulated Living Ziegler-Natta Polymerization. Angew. Chem., Int. Ed. 2006, 45, 6140-6144. (g) Zhang, W.; Sita, L. R. Investigation of Dynamic Intra- and Intermolecular Processes within a Tether-Length Dependent Series of Group 4 Bimetallic Initiators for Stereomodulated Degenerative Transfer Living Ziegler-Natta Propene Polymerization. Adv. Synth. Catal. 2008, 350, 439-447. (h) Crawford, K. E.; Sita, L. R. Stereoengineering of Poly(1,3-methylenecyclohexane) via Two-State Living Coordination Polymerization of 1,6- Heptadiene. J. Am. Chem. Soc. 2013, 135, 8778-8781. (i) Crawford, K. E.; Sita, L. R. Regio- and Stereospecific Cyclopolymerization of Bis(2-propenyl)diorganosilanes and the Two-State Stereoengineering of 3,5-Cis, Isotactic Poly(3,5methylene-1-silacyclohexane)s. ACS Macro Lett. 2014, 3, 506-509.
- (7) For an investigation of non-living degenerative transfer coordinative polymerization of α -olefins, see: Xiong, S.; Steelman, D. K.; Medvedev, G. A.; Delgass, W. N.; Abu-Omar, M. M.; Caruthers, J. M. Selective Degenerative Benzyl Group Transfer in Olefin Polymerization. *ACS Catal.* **2014**, *4*, 1162–1170.
- (8) For the use of LCP for the synthesis of well-defined polyolefin di- and triblock copolymers as thermoplastic elastomers, see, for instance: ref 6f and (a) Giller, C.; Gururajan, G.; Wei, J.; Zhang, W.; Hwang, W.; Chase, D. B.; Rabolt, J. F.; Sita, L. R. Synthesis, Characterization, and Electrospinning of Architecturally-Discrete Isotactic-Atactic-Isotactic Triblock Stereoblock Polypropene Elastomers. *Macromolecules* 2011, 44, 471–482. (b) Crawford, K. E.; Sita, L. R. De Novo Design of a New Class of "Hard-Soft" Amorphous, Microphase-Separated, Polyolefin Block Copolymer Thermoplastic Elastomers. *ACS Macro Lett.* 2015, 4, 921–925.
- (9) More specifically, $\mathrm{DP_n} = \{([\mathrm{monomer}]_t [\mathrm{monomer}]_0)/([\mathrm{M-P_a}] + z[\mathrm{M'-G}])\}$, where in the case of degenerative LCP, $[\mathrm{M-P_a}]$ and $[\mathrm{M'-G}]$ are the populations of transition-metal active and dormant species, respectively, z is the fraction of pre-initiator remaining after activation and $G = \mathrm{Me}$ (methyl group transfer). For the case of two-state LCCTP, $[\mathrm{M'-G}]$ is now the population of main-group-metal alkyl species, $G = \mathrm{P}$ (polymeryl transfer) and z is the number of equivalent groups of the latter that are involved in reversible chain transfer (i.e. z = 2 for $\mathrm{M'} = \mathrm{Zn}$). For a degenerative transfer living polymerization, $D = (\mathrm{M_w/M_n}) \approx 1 + k_\mathrm{p}/k_\mathrm{ex}$, where M_n and M_w are the number- and weight-average molecular weight indices, respectively.
- (10) Müller, A. H. E.; Zhuang, R.; Yan, D.; Litvinenko, G. Kinetic Analysis of "Living" Polymerization Processes Exhibiting Slow Equilibria. 1. Degenerative Transfer (Direct Activity Exchange

ACS Catalysis pubs.acs.org/acscatalysis Research Article

between Active and "Dormant" Species). Application to Group Transfer Polymerization. *Macromolecules* 1995, 28, 4326–4333.

- (11) Cueny, E. S.; Landis, C. R. Zinc-Mediated Chain Transfer from Hafnium to Aluminum in the Hafnium-Pyridyl Amido-Catalyzed Polymerization of 1-Octene Revealed by Job Plot Analysis. *Organometallics* **2019**, 38, 926–932.
- (12) Thomas, T. S.; Hwang, W.; Sita, L. R. End-Group-Functionalized Poly(α -olefinates) as Non-Polar Building Blocks: Self-Assembly of Sugar-Polyolefin Hybrid Conjugates. *Angew. Chem., Int. Ed.* **2016**, 55, 4683–4687.
- (13) (a) Nowak, S. R.; Hwang, W.; Sita, L. R. Dynamic Sub-10-nm Nanostructured Ultrathin Films of Sugar-Polyolefin Conjugates Thermoresponsive at Physiological Temperatures. J. Am. Chem. Soc. 2017, 139, 5281–5284. (b) Lachmayr, K. K.; Wentz, C. M.; Sita, L. R. An Exceptionally Stable and Scalable Sugar-Polyolefin Frank-Kasper A15 Phase. Angew. Chem., Int. Ed. 2020, 59, 1521–1526. (c) Lachmayr, K. K.; Sita, L. R. Small Molecule Modulation of Soft Matter Frank-Kasper Phases: A New Paradigm for Adding Function to Form. Angew. Chem., Int. Ed. 2020, 59, 3563–3567. (d) Nowak, S. R.; Lachmayr, K. K.; Yager, K. G.; Sita, L. R. Stable Thermotropic 3D and 2D Double Gyroid Nanostructures with Sub-2-nm Feature Size for Scalable Sugar-Polyolefin Conjugates. Angew. Chem., Int. Ed. 2021, 60, 8710–8716.
- (14) (a) Bochmann, M. The Chemistry of Catalyst Activation: The Case of Group 4 Polymerization Catalysts. *Organometallics* **2010**, *29*, 4711–4740. (b) Zaccaria, F.; Sian, L.; Zuccaccia, C.; Macchioni, A. Ion Pairing in Transition Metal Catalyzed Olefin Polymerization. *Adv. Organomet. Chem.* **2020**, *73*, 1–78.
- (15) Tran, T. V.; Do, L. H. Tunable Modalities in Polyolefin Synthesis via Coordination Insertion Polymerization. *Eur. Polym. J.* **2021**, *142*, 110100.
- (16) Experimental details are provided in the Supporting Information.
- (17) Keaton, R. J.; Jayaratne, K. C.; Fettinger, J. C.; Sita, L. R. Structural Characterization of Zirconium Cations Derived from a Living Ziegler-Natta Polymerization System: New Insights Regarding Propagation and Termination. *J. Am. Chem. Soc.* **2000**, *122*, 12909–12910.
- (18) (a) Rocchigiani, L.; Busico, V.; Pastore, A.; Talarico, G.; Macchioni, A. Unusual Hafnium-Pyridylamido/ER $_{\rm n}$ Heterobimetallic Adducts (ER $_{\rm n}$ = ZnR $_{\rm 2}$ or AlR $_{\rm 3}$). Angew. Chem., Int. Ed. 2014, 53, 2157–2161. (b) Rocchigiani, L.; Busico, V.; Pastore, A.; Macchioni, A. Comparative NMR Study on the Reaction of Hf(IV) Organometallic Complexes with Al/Zn Alkyls. Organometallics 2016, 35, 1241–1250.
- (19) See for instance: (a) Lynd, N. A.; Hillmyer, M. A. Influence of Polydispersity on the Self-Assembly of Diblock Copolymers. Macromolecules 2005, 38, 8803-8810. (b) Listak, J.; Jakubowski, W.; Mueller, L.; Plichta, A.; Matyjaszewski, K.; Bockstaller, M. R. Effect of Symmetry of Molecular Weight Distribution in Block Copolymers on Formation of "Metastable" Morphologies. Macromolecules 2008, 41, 5919-5927. (c) Plichta, A.; Zhong, M.; Li, W.; Elsen, A. M.; Matyjaszewski, K. Tuning Dispersity in Diblock Copolymers Using ARGET ATRP. Macromol. Chem. Phys. 2012, 213, 2659-2668. (d) Kottisch, V.; Gentekos, D. T.; Fors, B. P. "Shaping" the Future of Molecular Weight Distributions in Anionic Polymerization. ACS Macro Lett. 2016, 5, 796-800. (e) Gentekos, D. T.; Dupuis, L. N.; Fors, B. P. Beyond Dispersity: Deterministic Control of Polymer Molecular Weight Distribution. J. Am. Chem. Soc. 2016, 138, 1848-1851. (f) Corrigan, N.; Almasri, A.; Taillades, W.; Xu, J.; Boyer, C. Controlling Molecular Weight Distributions through Photoinduced Flow Polymerization. Macromolecules 2017, 50, 8438-8448. (g) Gentekos, D. T.; Jia, J.; Tirado, E. S.; Barteau, K. P.; Smilgies, D.-M.; DiStasio, R. A., Jr.; Fors, B. P. Exploiting Molecular Weight Distribution Shape to Tune Domain Spacing in Block Copolymer Thin Films. J. Am. Chem. Soc. 2018, 140, 4639-4648. (h) Spinnrock, A.; Cölfen, H. Control of Molar Mass Distribution by Polymerization in the Analytical Ultracentrifuge. Angew. Chem., Int. Ed. 2018, 57, 8284-8287. (i) Whitfield, R.; Parkatzidis, K.; Rolland, M.; Truong, N.

- P.; Anastasaki, A. Tuning Dispersity by Photoinduced Atom Transfer Radical Polymerization: Monomodal Distributions with ppm Copper Concentration. Angew. Chem., Int. Ed. 2019, 58, 13323-13328. (j) Walsh, D. J.; Guironnet, D. Macromolecules with Programmable Shape, Size, and Chemistry. Proc. Natl. Acad. Sci. U.S.A. 2019, 116, 1538-1542. (k) Rubens, M.; Junkers, T. A Predictive Framework for Mixing Low Dispersity Polymer Samples to Design Custom Molecular Weight Distributions. Polym. Chem. 2019, 10, 5721-5725. (1) Rubens, M.; Junkers, T. Comprehensive Control over Molecular Weight Distributions through Automated Polymerizations. Polym. Chem. 2019, 10, 6315-6323. (m) Whitfield, R.; Parkatzidis, K.; Truong, N. P.; Junkers, T.; Anastasaki, A. Tailoring Polymer Dispersity by RAFT Polymerization: A Versatile Approach. Chem 2020, 6, 1340-1352. (n) Rolland, M.; Truong, N. P.; Whitfield, R.; Anastasaki, A. Tailoring Polymer Dispersity in Photoinduced Iron-Catalyzed ATRP. ACS Macro Lett. 2020, 9, 459-463. (o) Walsh, D. J.; Schinski, D. A.; Schneider, R. A.; Guironnet, D. General Route to Design Polymer Molecular Weight Distributions through Flow Chemistry. Nat. Commun. 2020, 11, 3094. (p) Liu, H.; Xue, Y.-H.; Zhu, Y.-L.; Gu, F.-L.; Lu, Z.-Y. Inverse Design of Molecular Weight Distribution in Controlled Polymerization via a One-Pot Reaction Strategy. Macromolecules 2020, 53, 6409-6419. (q) Liu, K.; Corrigan, N.; Postma, A.; Moad, G.; Boyer, C. A Comprehensive Platform for the Design and Synthesis of Polymer Molecular Weight Distributions. Macromolecules 2020, 53, 8867-8882. (r) Rosenbloom, S. I.; Fors, B. P. Shifting Boundaries: Controlling Molecular Weight Distribution Shape for Mechanically Enhanced Thermoplastic Elastomers. Macromolecules 2020, 53, 7479-7486. (s) Sifri, R. J.; Padilla-Vélez, O.; Coates, G. W.; Fors, B. P. Controlling the Shape of Molecular Weight Distributions in Coordination Polymerization and Its Impact on Physical Properties. J. Am. Chem. Soc. 2020, 142, 1443-1448. (t) Rosenbloom, S. I.; Sifri, R. J.; Fors, B. P. Achieving Molecular Weight Distribution Shape Control and Broad Dispersities using RAFT Polymerizations. Polym. Chem. 2021, DOI: 10.1039/ d1py00399b.
- (20) Wallace, M. A.; Sita, L. R. Temporal Control over Two- and Three-State Living Coordinative Chain Transfer Polymerization for Modulating the Molecular Weight Profile of Polyolefins. *Angew. Chem., Int. Ed.* **2021**, *60.* DOI: 10.1002/anie.202105937.